

Drivers of genomic landscapes of differentiation across *Populus* divergence gradient

Huiying Shang^{1,2,3*}, Martha Rendón-Anaya⁴, Ovidiu Paun¹, David L Field⁵, Jaqueline Hess⁶,
Claus Vogl⁷, Jianquan Liu⁸, Pär K. Ingvarsson⁴, Christian Lexer^{1,10†}, Thibault Leroy^{1,9,10*}

¹Department of Botany and Biodiversity Research, University of Vienna, Vienna, Austria.

²Vienna Graduate School of Population Genetics, Vienna, Austria.

³Xi'an Botanical Garden, Shaanxi Academy of Sciences, Shaanxi, People's Republic of China.

⁴Swedish University of Agricultural Sciences (SLU), Uppsala, Sweden.

⁵Edith Cowan University, Perth, Australia.

⁶Helmholtz Centre for Environmental Research, Halle (Saale), Germany.

⁷Department of Biomedical Sciences, Vetmeduni Vienna, Vienna, Austria

⁸Key Laboratory for Bio-resources and Eco-environment, College of Life Science, Sichuan University, Chengdu, People's Republic of China

⁹IRHS-UMR1345, Université d'Angers, INRAE, Institut Agro, SFR 4207 QuaSaV, 49071 Beaucouzé, France

¹⁰Shared last authorship.

†Deceased.

*Corresponding authors:

- Thibault Leroy, Department of Botany and Biodiversity Research, University of Vienna,
Rennweg 14, 1030 Vienna, Austria

Email: thibault.leroy@univie.ac.at

- Huiying Shang, Xi'an Botanical Garden, Shaanxi Academy of Sciences, Shaanxi, People's
Republic of China.

Email: shanghuiying@outlook.com

Abstract

Speciation, the continuous process by which new species form, is often investigated by looking at the variation of nucleotide diversity and differentiation across the genome (hereafter genomic landscapes). A key challenge lies in how to determine the main evolutionary forces at play shaping these patterns. One promising strategy, albeit little used to date, is to comparatively investigate these genomic landscapes as a progression through time by using a series of species pairs along a divergence gradient. Here, we resequenced 201 whole-genomes from eight closely related *Populus* species, with pairs of species at different stages along the speciation gradient to learn more about divergence processes. Using population structure and ancestry analyses, we document extensive introgression between some species pairs, especially those with parapatric distributions. We further investigate genomic landscapes, focusing on within-species (nucleotide diversity and recombination rate) and among-species (relative and absolute divergence) summary statistics of diversity and divergence. We observe highly conserved patterns of genomic divergence across species pairs. Independent of the stage across the divergence gradient, we find support for signatures of linked selection (i.e., the interaction between natural selection and genetic linkage) in shaping these genomic landscapes, along with gene flow and standing genetic variation. We highlight the importance of investigating genomic patterns on multiple species across a divergence gradient and discuss prospects to better understand the evolutionary forces shaping the genomic landscapes of diversity and differentiation.

Keywords: differentiation islands, divergence, introgression, identity-by-descent, linked selection, recombination

Introduction

Understanding the evolutionary forces that shape genetic variation is a central goal of biology. Numerous population genomic studies have recently documented variation of the levels of within-species genetic diversity and among-species differentiation across the genome (hereafter genomic landscapes). Most frequently, these studies point to a highly heterogeneous nature of these landscapes, leading to further investigations into the evolutionary forces

responsible for genomic regions of elevated and reduced differentiation between diverging populations or species (Ellegren, et al. 2012; Martin, et al. 2013; Lamichhaney, et al. 2015; Vijay, et al. 2016; Sendell-Price, et al. 2020).

Hotspots of elevated genetic differentiation relative to genomic background are often referred to as ‘differentiation islands’ or ‘speciation islands’ and are assumed to form around loci underlying local adaptation and/or reproductive isolation. Thus, delineating differentiation islands has recently become a major topic of research in the field of speciation and adaptation genomics (Burri 2017b; Martin and Jiggins 2017; Ravinet, et al. 2018; Tavares, et al. 2018; Stankowski, et al. 2019). Such investigations are best suited for groups still experiencing interspecific gene flow, *i.e.*, species diverging under an isolation-with-migration or a secondary contact scenario (Harrison and Larson 2016; Roux, et al. 2016; Wolf and Ellegren 2017; Leroy, et al. 2020; Yamasaki, et al. 2020). Genomic regions containing barrier loci are more resistant to gene flow and are therefore expected to show higher levels of differentiation (the islands) as compared to the rest of the genome (the sea level, Wu 2001). A number of empirical studies in plants have proved the joint role of gene flow and selection in shaping these highly heterogeneous genomic landscapes of differentiation and identified reproductive isolation genes (*e.g.* Tavares, et al. 2018; Martin, et al. 2019; Stankowski, et al. 2019).

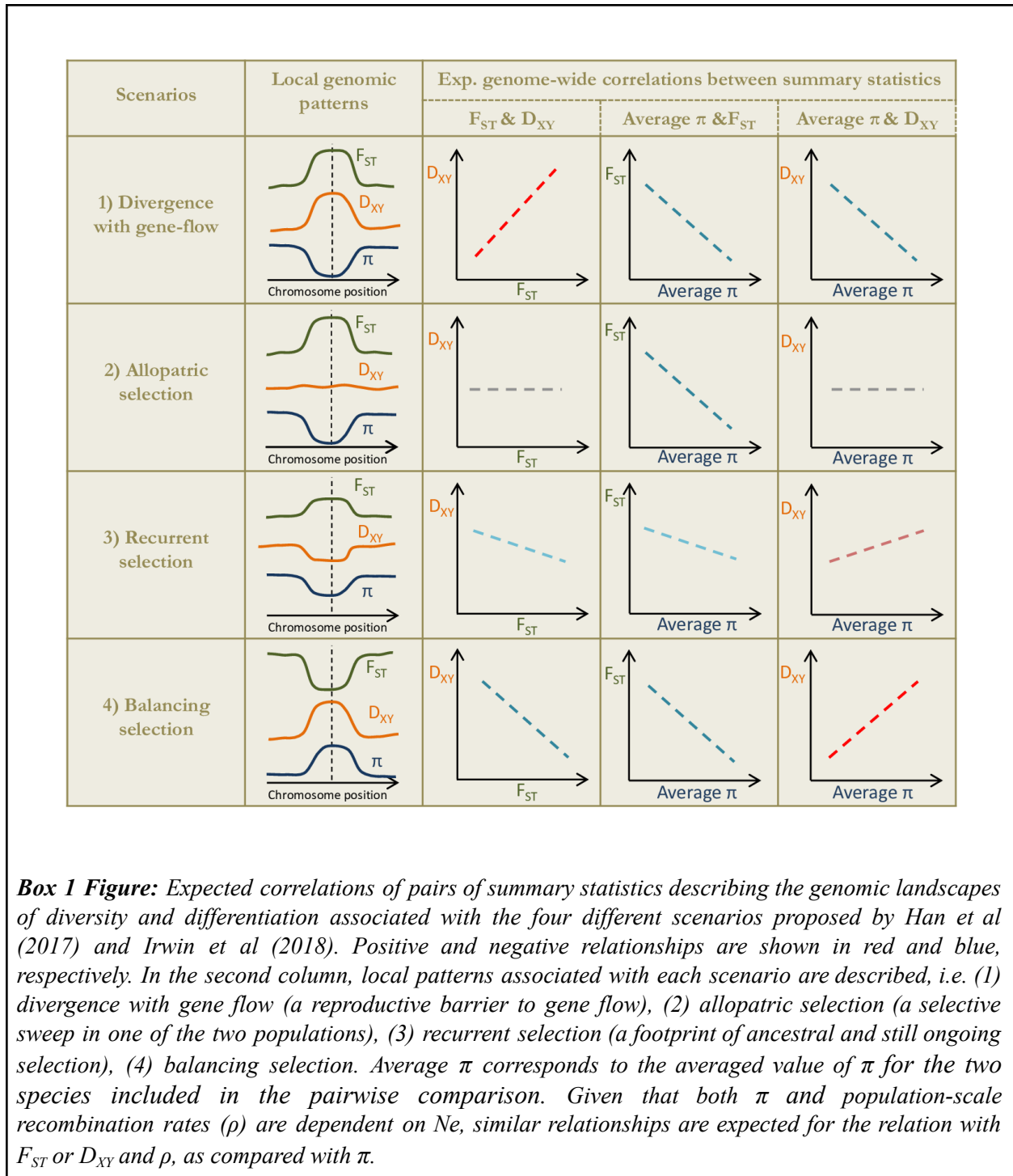
Heterogeneous differentiation landscapes can however also emerge due to other genomic features not causally linked to reproductive barriers and speciation (Booker and Keightley 2018). Linked selection, the interaction between natural selection and genetic linkage may contribute to these diversity and differentiation landscapes. Two forms of linked selection are generally recognised: background selection and genetic hitchhiking; although their relative importance is still debated (Stephan 2010). Background selection (Charlesworth, et al. 1993), the effect of natural selection against deleterious alleles at linked neutral polymorphism, is known to reduce diversity, particularly in regions with relatively high gene density (Corbett-Detig, et al. 2015; Wolf and Ellegren 2017). Similarly, due to genetic hitchhiking, neutral alleles are dragged along with positively selected ones (Smith and Haigh 1974). Linked selection reduces effective population size (N_e) and can lead to regions of decreased diversity and elevated relative

differentiation. In regions of low recombination, linked selection can generate footprints that extend over larger genomic regions around the positively or negatively selected loci (Charlesworth and Campos, 2014). Thus, nucleotide diversity (*e.g.*, π) and relative differentiation (*e.g.*, F_{ST}) estimates are expected to be negatively correlated (Burri 2017a). Such correlations have been reported in *Ficedula* flycatchers (Burri, et al. 2015), *Heliconius* (Edelman, et al. 2019; Martin, et al. 2019; Van Belleghem, et al. 2021), *Helianthus* sunflowers (Renaut, et al. 2013), the Pacific cupped oyster (Gagnaire, et al. 2018), warblers (Irwin, et al. 2018), and hummingbirds (Henderson and Brelsford 2020).

To understand the processes behind the heterogeneous differentiation landscapes along a divergence gradient, a suite of summary statistics, widely used in population genomics, has been employed (Han, et al. 2017; Irwin, et al. 2018). These summary statistics include (i) the average nucleotide diversity within populations (π), (ii) the relative differentiation between populations (F_{ST}) and (iii) the absolute divergence between populations (D_{XY}) (see Box 1).

Box 1: Correlations of genomic landscapes under different scenarios of divergence

Following Han *et al* (2017) and Irwin *et al* (2018) four main evolutionary scenarios can be hypothesized. The first scenario is ‘divergence with gene flow’ where selection at loci contributing to reproductive isolation restricts gene exchange between diverging species, locally elevating genomic differentiation (leading to both high F_{ST} and D_{XY}) and reducing genetic diversity. The second scenario is ‘allopatric selection’ where linked selection occurs independently within each species after the split leading locally to lower π and higher F_{ST} . Allopatric selection has opposite effects on D_{XY} , leaving it quite unchanged in combination. The third scenario is ‘recurrent selection’ where the same selective pressure reduces diversity at selected and linked loci leading to lower polymorphism within populations but similar divergence, *ie.* relatively low π and D_{XY} due to its dependence on ancestral polymorphism and high F_{ST} . The fourth and last scenario is ‘balancing selection’ where ancestral polymorphism is maintained between nascent species, resulting in elevated genetic diversity and low genetic differentiation. Then π is expected to be higher than neutral (as is D_{XY} , due to the high ancestral diversity) while F_{ST} is expected to be low.



In this study, we focused on white poplars and aspens from the section *Populus* within the genus *Populus*. These trees are widely distributed in Eurasia and North America (Supporting Fig. S1 and Table S1) and provide a set of species pairs along the continuum of divergence.

Divergence times among species pairs vary from 1.3 to 4.8 million years ago (Shang, et al. 2020). This provides an excellent system to investigate the evolution of genomic landscapes of diversity and divergence through time and to better understand the relative contribution of different evolutionary processes to genomic landscapes. We use whole genome resequencing data from eight *Populus* species (Supporting Fig. S1 and Table S1) to address the following questions: (1) How do genomic landscapes of differentiation accumulate along the divergence gradient? (2) Are differentiation patterns across the genomic landscape repeatable among independent lineages? (3) What are the main evolutionary processes driving these heterogeneous landscapes of diversity and differentiation along the divergence gradient? (4) Which divergence scenario is consistent with ‘differentiation islands’ in each species pair?

Results and Discussions

Strong interspecific structure despite interspecific introgression

A large dataset of 30,539,136 high-quality SNPs was obtained by identifying SNPs among individuals from seven *Populus* species (after the exclusion of *P. qionghoensis*, see Materials and Methods). Neighbor-joining (Fig. 1a) and admixture analyses (based on a subset of 85,204 unlinked SNPs, Fig. 1b and Supporting Figs. S4 and S5) identified seven genetic groups, which were consistent with previously identified species boundaries based on phylogenomic analyses (Shang et al, 2020). Additionally, Admixture also indicated potential introgression between the subtropical species *P. adenopoda* and two recently diverged species, *P. davidiana* and *P. rotundifolia* (Fig. 1b and Supporting Fig. S5). Identity-by-descent (IBD) analyses (Fig. 1c) also identified seven reliable clusters, corresponding to the same species boundaries, but further pinpointed some shared haplotypes among the aspen species *P. davidiana*, *P. rotundifolia* and *P. tremula*, indicating recent introgression or incomplete lineage sorting among these species. The IBD results also provide support for extensive introgression between two pairs of highly divergent species with overlapping distributions, including *P. alba* and *P. tremula*, and also *P. grandidentata* and *P. tremuloides*. These results suggest a scenario of divergence with ongoing gene flow for some species pairs, either due to isolation-with-migration or secondary contact,

maintained even after substantial divergence times (net divergence d_a : 0.023 for *P. alba* - *P. tremula*; d_a : 0.025 for *P. tremuloides* - *P. grandidentata*).

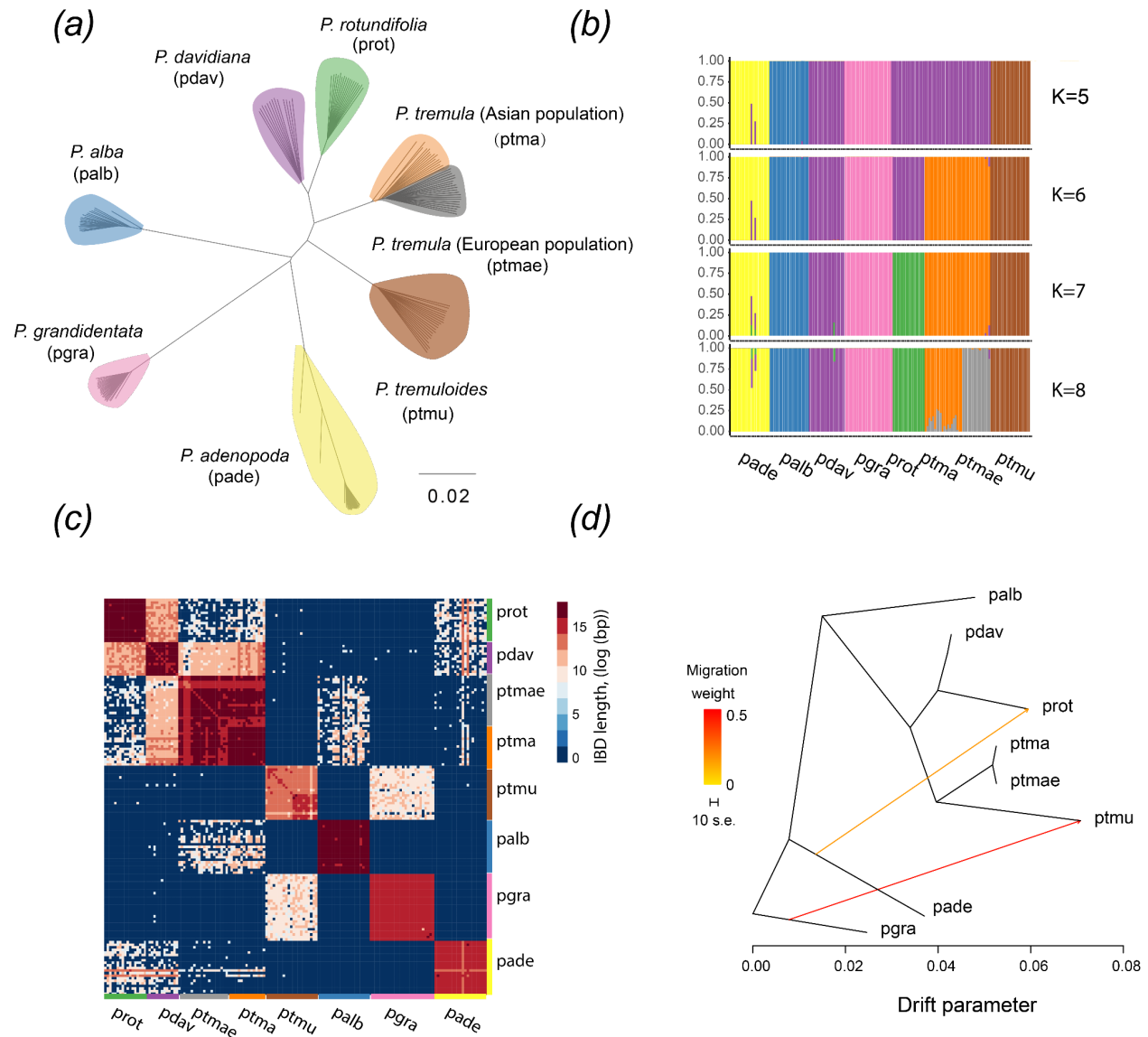


Figure 1. Genetic structure among *Populus* (poplar and aspen) accessions investigated. **(a)** Neighbor-joining tree based on all SNPs for seven *Populus* species. Colored clusters represent different species according to legend. **(b)** Estimated membership of each individual's genome for $K = 5$ to $K = 8$ as estimated by Admixture (best $K = 7$). **(c)** Identity by descent (IBD) analysis for seven *Populus* species. Heatmap colours represent the shared haplotype length between species. **(d)** The maximum likelihood tree inferred by TreeMix under a strictly bifurcating model with two migration events.

We have further confirmed that the tree topology recovered with TreeMix (Pickrell and Pritchard 2012) was consistent with phylogenetic relationships found in a previous study (Shang, et al. 2020). This expected main topology explained 95.8% of the total variance under a drift-only model of divergence. In addition, TreeMix was used to infer putative migration events in *Populus* (Fig. 1d). Adding a single migration edge allowed us to account for 98.9% of the total variance (Supporting Fig. S6). This event was inferred from *P. grandidentata* to *P. tremuloides* and is consistent with previous reports of extensive hybridization and introgression between these two species (Deacon, et al. 2019). A second migration edge was inferred from *P. adenopoda* to *P. rotundifolia*, which allowed us to explain 99.6% of the total variance (Fig. 1d). By adding more migration edges, the variance explained plateaued (increasing by less than 0.1%, which was considered as too marginal, Supporting Fig. S6). Therefore, we considered the bifurcating tree with two migration events as the best scenario in this analysis explaining the historical relationships among these *Populus* species based on our data and sampling.

Detecting local genomic patterns consistent with the four scenarios

Using non-overlapping 10kb sliding windows spanning the genome, we reported diversity and divergence estimates for all species and species pairs (Fig. 2a). Mean F_{ST} varied from 0.23 between *P. davidiana* - *P. rotundifolia* to 0.71 between *P. adenopoda* - *P. grandidentata*, whereas D_{XY} ranged from 0.016 (*P. davidiana* - *P. rotundifolia*) to 0.028 (*P. adenopoda* - *P. grandidentata*). The average π varied from 3.5×10^{-3} in *P. grandidentata* to 8.4×10^{-3} in *P. tremuloides* (Fig. 2a). The relatively high average π value observed in *Populus* species is consistent with the large SMC++-inferred effective population sizes for these species (Supplementary Note 1) and the fast LD decay (Supporting Fig. S7). In addition to nucleotide diversity and differentiation across 10kb sliding windows, we also computed ρ . Since both π and ρ scale with N_e , significant correlations of the diversity and recombination landscapes were expected and were indeed empirically observed for each species (correlations ranging from 0.12 for *P. adenopoda* and 0.23 for *P. davidiana*).

We then identified regions that could be consistent with the alternative divergence scenarios (described in Box 1) for five representative species pairs (Supporting Fig. S8). These species pairs were selected to represent distinct stages across the divergence gradient, from early to late stages of speciation (blue labels in Fig. 2a). Our results are consistent with a heterogeneous distribution of the four scenarios along the genome for all five species pairs (Fig. 2b, see also Supporting Fig. S9-S13 and Table S2). This generates different genome-wide patterns of correlations among species pairs, rather than a single scenario at play across the whole genome (Fig. 2c, Box 1). The majority of the genome (74.3%-78.7%) in all five species pairs fits a scenario of “allopatric selection”, in which the excess of F_{ST} was driven by low π and not higher D_{XY} (rosa bars in Fig. 2b, Supporting Fig. S9-S13 and Table S2). Such a signature is consistent with recent footprints of positive or background selection on genomic differentiation and is therefore consistent with the hypothesis of a prime role of linked selection (see also Supplementary Note 2 for an explicit detection of selective sweeps). Genomic regions fitting the scenario of ‘balancing selection’ (scenario d in Supporting Fig. S8) are the second most frequent for all investigated species pairs (11.6%-13.9% of detected regions). This scenario is characterized by an elevated D_{XY} but a low F_{ST} implying the action of balancing selection in shaping the heterogeneous landscape of divergence. In addition, we found support for divergence-with-gene flow in all five species pairs (5.5%-8.1%), suggesting that genomic heterogeneity in the levels of gene flow due to species barriers play a role in shaping genomic differentiation landscapes. Interestingly, this result holds true for all five species pairs we investigated in detail, *i.e.*, regardless of the level of gene flow or the stage along the *Populus* speciation continuum. Indeed, limited gene flow was inferred between *P. adenopoda* - *P. alba*, but regions with high D_{XY} were also identified in this highly diverged species pair and could be rather due to shared ancestral polymorphisms. In contrast, at the early stage of divergence, local barriers to gene flow may play an important role in genomic heterogeneous divergence, as significantly positive correlations between D_{XY} and F_{ST} are found (Fig. 3c), which is consistent with a divergence with gene-flow scenario (Box 1 figure). Besides, for early stages of divergence background selection may have too limited power to explain alone regional patterns of accentuated differentiation (Burri 2017b).

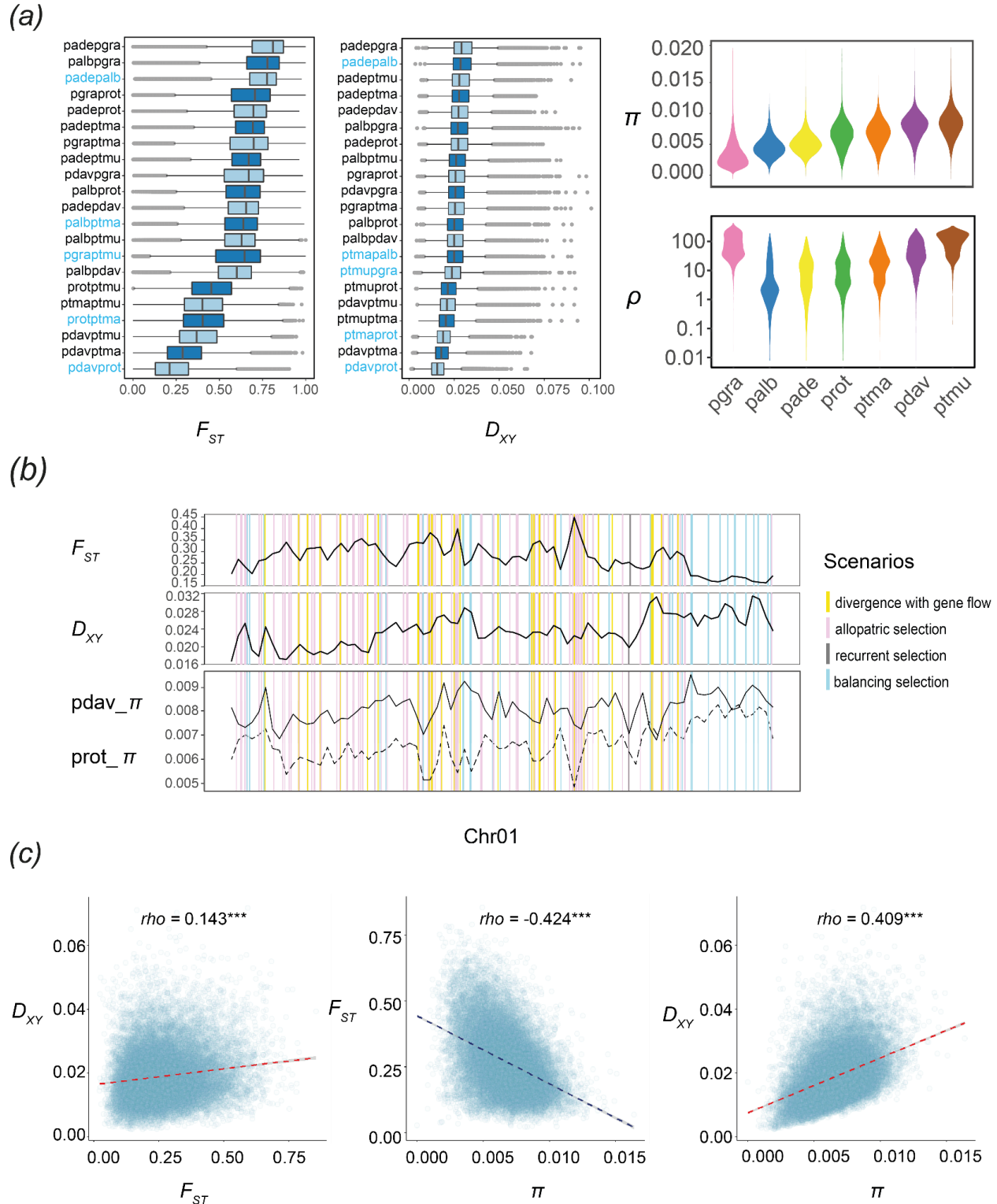


Figure 2. (a) Observed variance in F_{ST} , D_{XY} for all species pairs, and π and ρ for seven *Populus* species, calculated across 10kb windows. The five representative species pairs were labeled in blue. Note that the

unit of ρ is $4Ner$ and that ρ is log-scaled. **(b)** Landscapes of π , F_{ST} , and D_{XY} on chromosome 1 for the two closest species, *P. davidiana* and *P. rotundifolia*. **(c)** Genome-wide correlation analysis for π , F_{ST} , D_{XY} and ρ between *P. davidiana* and *P. rotundifolia*. *P* values less than 0.001 are summarized with three asterisks.

Conserved genomic landscapes across the continuum of divergence

We calculated genome-wide correlations of divergence, nucleotide diversity, and recombination across non-overlapping 10kb windows spanning the whole genome between pairwise comparisons of species or species pairs (Fig. 2a). The degree of correlation of both the relative and absolute divergence landscapes between pairs of species supports a highly conserved pattern among the five investigated species pairs (Fig. 3a-b, between *P. adenopoda* -*P. alba* and *P. tremula* -*P. alba* for F_{ST} and between *P. rotundifolia* - *P. davidiana* and *P. rotundifolia* - *P. tremula* for D_{XY}). The correlations of F_{ST} landscapes become stronger when the overall differentiation increases. For instance, the correlation of F_{ST} between *P. tremula* - *P. alba* and *P. rotundifolia* - *P. davidiana* is 0.24, while the value for the two most divergent species pairs (between *P. adenopoda* - *P. alba* and *P. tremuloides* - *P. grandidentata*) is 0.56. This may be the case that the effect of linked selection accumulates as differentiation advances. Comparing landscapes of the nucleotide diversity π between species (Fig. 3c), we observed that the correlation coefficients vary substantially, from 0.16 (*P. tremula* versus *P. grandidentata*) to 0.52 (*P. rotundifolia* versus *P. davidiana*). The correlation generally decreases with the phylogenetic distance. We notably reported the strongest correlation coefficient for the phylogenetically closest pair of species: *P. rotundifolia* and *P. davidiana* (Fig. 3c). Pairwise comparisons of the local recombination rates inferred independently for all species also revealed only positive correlations (Fig. 3d), with the highest positive correlation coefficient of ρ again observed between the two closest related species, *P. davidiana* and *P. rotundifolia* (0.47), while the weaker correlation was observed for *P. davidiana* and *P. grandidentata* (0.08). Most of the lower values (correlation coefficients < 0.2) were found when comparing *P. grandidentata* with other species, suggesting again a unique recombination landscape in this species. Interestingly, correlations of π were in general higher than those of ρ , indicating that not only recombination rate variation shapes nucleotide diversity. Overall, landscapes of genetic diversity, divergence and

recombination rate remain relatively stable across different species or species pairs (Fig. 3), which implies relatively conserved genomic features across all species. This phenomenon has also been observed in few other plant and animal model systems (Nosil and Feder 2012; Renault, et al. 2014; Burri, et al. 2015; Wang, et al. 2020).

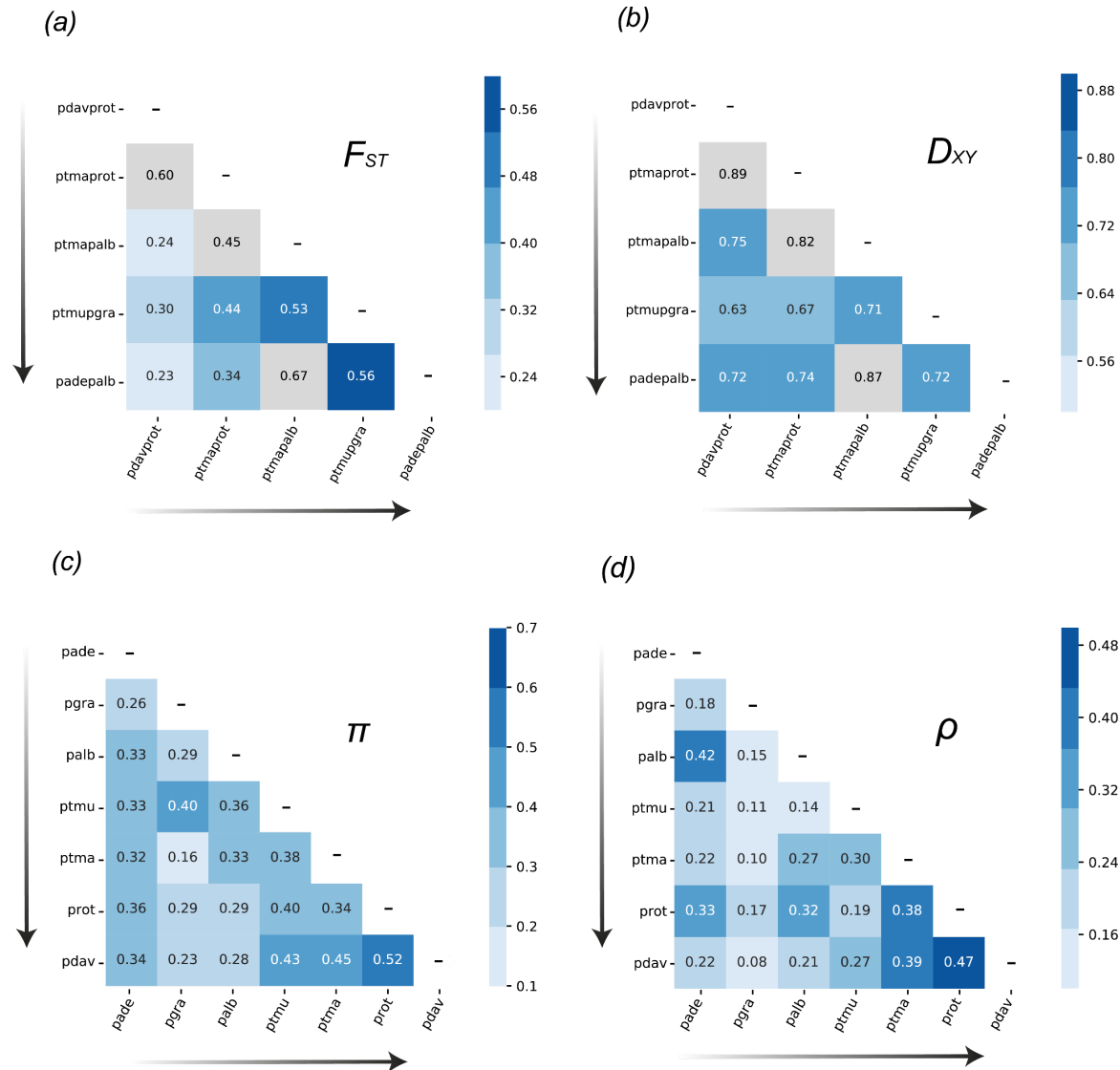


Figure 3. Correlations analyses of within-species diversity or among-species divergence landscapes (a-b) Correlation coefficients of F_{ST} or D_{XY} between species pairs. The species pairs are ordered across the divergence gradient (arrows). Comparisons containing a shared species were masked (grey squares).

(c-d) Correlation coefficients of π or ρ between species. The order of the species is based on the order of species divergence from the root. All the values are significantly positively correlated ($p < 0.001$).

Correlated patterns of genome-wide variation across the *Populus* continuum of divergence

The conserved genomic patterns observed across independent species pairs indicates the role of linked selection in shaping genomic landscapes of differentiation (Fig. 3), in which background selection could play a major role, as deleterious mutations are much more common than beneficial ones. We then test if background selection may have driven these patterns alone. According to a generally accepted expectation proposed by Burri (2017b), the correlations between genomic variation and genome features should be impacted by background selection. First, the correlation between F_{ST} and ρ becomes stronger with divergence, as lineage-specific effects of background selection accumulate with time. Second, D_{XY} and π are highly correlated with one another under BGS, because diversity can be inherited from ancestors, being passed down over lineage splits. Third, π and ρ remain highly correlated, because background selection continues to play a role in the daughter populations after speciation.

The use of several species across a continuum of divergence allows us to evaluate how the correlations evolve through this continuum, from early to late stages of speciation. To this end, we used the level of genetic distance between each species pair (d_a : D_{XY} – mean π) as a proxy for the divergence time and we reported linear relationships between correlation coefficients across the 21 species pairs (Fig. 4). However, the correlation analysis between genomic variation and recombination rate showed different patterns from expectations under background selection. We found negative relationships between F_{ST} and ρ , but no significant changes associated with time since divergence (Fig. 4a). This is inconsistent with expectations under background selection (Burri 2017b). Similar investigations for π and F_{ST} showed significantly negative correlations while the trend became stronger as divergence increases (Fig. 4b). We also recovered a strong positive correlation between π and ρ (Fig. 4c), and a similar trend was found as for the investigation of π and D_{XY} (Fig. 4d). This trend is inconsistent with the general hypothesis that such correlations should remain highly correlated as divergence increases (Burri 2017b). For each species, we detected significant negative correlations between gene density and π in all

other *Populus* species (Supporting Fig. S14). The consistency is either due to background selection or genetic hitchhiking (Nordborg, et al. 2005; Stephan 2010). Pairwise correlations between D_{XY} and F_{ST} were significantly positive across the entire divergence continuum, and these correlations tend to become weaker as divergence increases (Fig. 4e). The observed patterns differ from expectations under a simple scenario with background selection as the sole factor shaping the heterogeneous landscape of differentiation across species, indicating that additional evolutionary factors contribute to the observed signal (Burri 2017b). Our analyses indicate that extensive gene flow and incomplete lineage sorting may contribute to differentiation landscapes as well, in particular in the early stages of the speciation continuum. However, with increasing divergence, the reduced gene flow and limited shared standing genetic variation may contribute less to differentiation landscapes. Consistent with our findings, studies in monkey flowers, threespine stickleback, and avian species also suggest that background selection may be too subtle to drive alone conserved genomic patterns across multiple species (Irwin, et al. 2018; Stankowski, et al. 2019; Rennison, et al. 2020). Indeed, these studies indicate either adaptive introgression or shared standing genetic variation also play major roles in generating similar patterns of genomic differentiation.

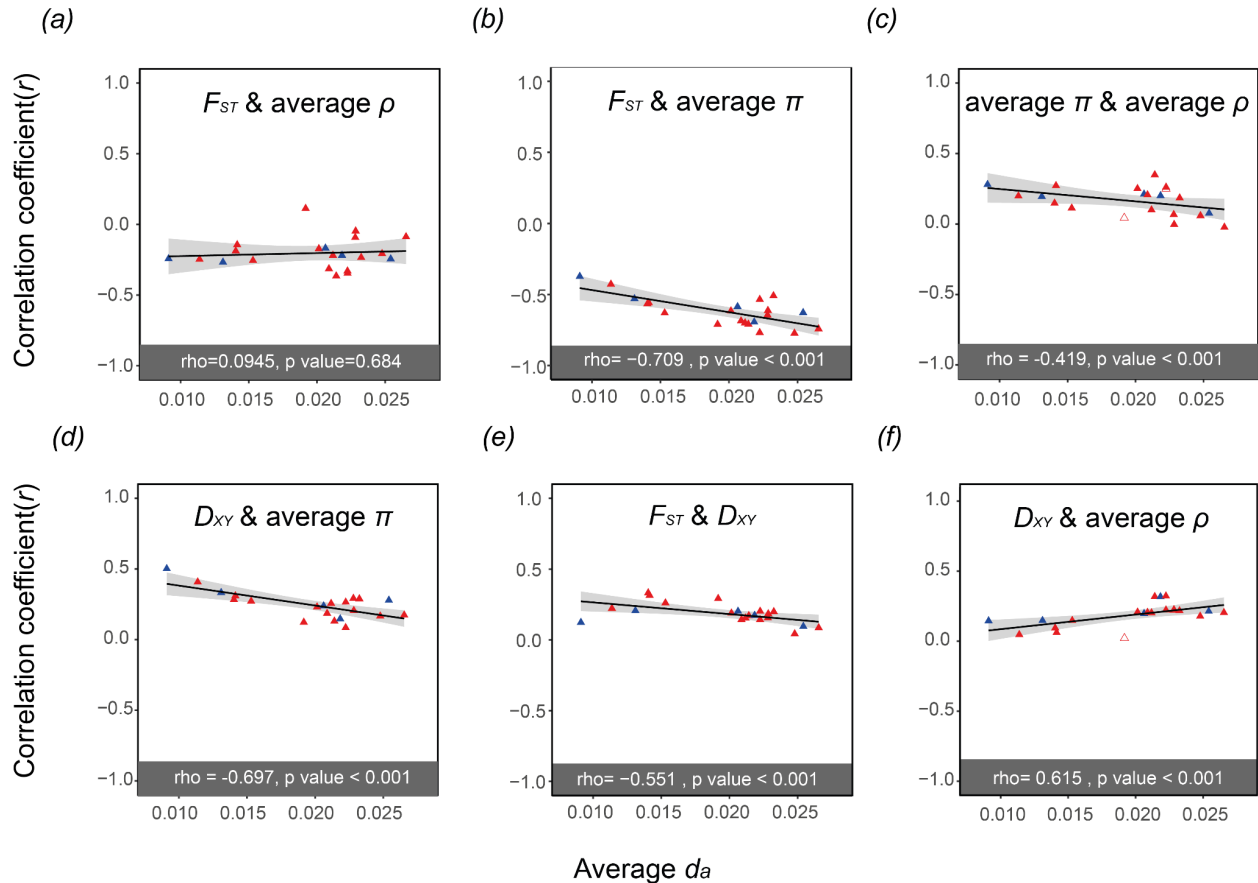


Figure 4. Correlations between variables for all species comparisons plotted against the averaged d_w used here as a measure of divergence time. The filled triangles indicate when the correlation coefficients are significant ($p < 0.01$). The blue triangles correspond to the correlation coefficients of the five representative species pairs shown in Fig. 2a and 3a-b. The results for all the other species pairs are shown in red. The upper panels show how the relationships between F_{ST} and (a) D_{XY} , or (b) average π vary for pairs of species with increasing divergence time; and between average π and D_{XY} for all species pairs investigated (c). The lower panels show how the relationships between average ρ and (d) F_{ST} , and (e) D_{XY} , and (f) average π vary for pairs of species with increasing divergence time.

Conclusions

In this study, we investigated the evolution of the genomic landscape across a divergence time continuum of seven species of *Populus*. By investigating evolution of diversity and differentiation landscapes across this divergence continuum, we provide a valuable case-study in terms of the number of species pairs analyzed (see also Stankowski, et al. 2019). Our analyses

support the primary role of linked selection, in particular background selection in shaping the empirical patterns of genomic differentiation, but its contribution alone is not sufficient to maintain the general consistency between these genomic landscapes. The observed positive correlations between F_{ST} and D_{XY} in all species pairs indicate that shared ancient polymorphism must also play a very important role. Besides, our study also confirmed the importance of gene flow in this plant system. We observed extensive introgression among species with parapatric distributions, despite a high level of divergence among the most divergent hybridizing species ($d_a = 0.025$). This is notable since the net divergence values are larger than the upper boundary for the ‘grey zone of speciation’ reported by Roux et al. (2016) for both vertebrate and invertebrate animals (d_a from 0.005 to 0.02). Further investigations across divergence continua in other plant systems are needed to determine if this is a general pattern in plants, or a feature of the specific demographic and evolutionary history of the *Populus* system. In the future, the investigation of speciation along multiple species complexes, together with the inclusion of the different scenarios of selection in more sophisticated demographic modeling approaches could represent a major step forward to provide a better description of the processes at play.

Materials and methods

Sampling, sequencing and read processing

Species of the genus *Populus* are perennial woody plants, dioecious, and widely distributed across the Northern Hemisphere (Stettler, et al. 1996). The genus *Populus* comprises six sections containing 29 species, among which ten species form the section *Populus* (Stettler, et al. 1996; Jansson, et al. 2010). The genus *Populus* is well studied not only due to the trees' economic and ecological importance, but also due to their small genome sizes (<500Mb), diploidy through the genus ($2n = 38$), wind pollination, extensive gene flow among species, and sexual and vegetative reproductive strategies (Rajora and Dancik 1992; Martinsen, et al. 2001; Suarez-Gonzalez, et al. 2016). Among all woody perennial angiosperm species, the genome of *Populus trichocarpa* was sequenced and published first (Tuskan, et al. 2006). In addition to *P. trichocarpa*, another well-annotated genome assembly is available (*P. tremula*; Schiffthaler, et al. 2019).

Two hundred and one samples were collected from eight species of *Populus* section *Populus* in Eurasia and North America (supplemental material, Fig. S1 and Table S1). The leaves were dried in silica gel first and were then used for genomic DNA extraction with Plant DNeasy Mini Kit (Qiagen, Germany). To increase the purity of total DNA, we used the NucleoSpin gDNA Clean-up kit (Macherey-Nagel, Germany). Whole genome resequencing was performed with 2 x 150bp paired-end sequencing technology on Illumina HiSeq 3000 sequencer at the Institute of Genetics, University of Bern, Switzerland.

All raw sequencing reads were mapped to the *P. tremula* 2.0 reference genome (Schiffthaler, et al. 2019) using BWA-MEM, as implemented in bwa v0.7.10 (Li 2013). Samtools v1.3.1 was used to remove alignments with mapping quality below 20 (Li, et al. 2009). Read-group information including library, lane, sample identity and duplicates was recorded using Picard v2.5 (<http://broadinstitute.github.io/picard/>). Sequencing reads around insertions and deletions (*i.e.*, indels) were realigned using RealignerTargetCreator and IndelRealigner in the Genome Analysis Toolkit (GATK v3.6) (DePristo, et al. 2011). We used the GATK HaplotypeCaller and then GenotypeGVCFs for individual SNP calling and for joint genotyping, respectively, among

all samples using default parameters. Finally, we performed several filtering steps using GATK to retain only high-quality SNPs: (1) 'QD' < 2.0; (2) 'FS > 60.0'; (3) 'MQ < 40.0'; (4) 'ReadPosRankSum < -8.0'; (5) 'SOR > 4.0'; (6) 'MQRankSum < -12.5'. Moreover, we also excluded loci with missing data of more than 30% and discarded two individuals with very low depth of coverage (< 10), as calculated using VCFtools v0.1.15 (http://vcftools.sourceforge.net/man_latest.html). The scripts for SNP calling are available at <https://doi.org/10.5281/zenodo.6785344>.

Family relatedness and population structure analysis

To avoid pseudoreplication due to the inclusion of clone mates, we estimated kinship coefficients using the KING toolset for family relationship inference based on pairwise comparisons of SNP data (<http://people.virginia.edu/~wc9c/KING/manual.html>). The software classifies pairwise relationships into four categories according to the estimated kinship coefficient: a negative kinship coefficient estimation indicates the lack of a close relationship. Estimated kinship coefficients higher than >0.354 correspond to duplicates, while coefficients ranging from [0.177, 0.354], [0.0884, 0.177] and [0.0442, 0.0884] correspond to 1st-degree, 2nd-degree, and 3rd-degree relationships, respectively. This analysis identified 13 duplicated genotypes out of a total of 32 samples from the Korean population of *P. davidiana*. In addition, all individuals of *P. qionghdaoensis* were identified as clone mates (supplementary material, Fig. S2). Therefore, these two populations were eliminated from subsequent analyses and only 7 species were kept for the analyses.

After discarding individuals with low depth and high inbreeding coefficient ($F > 0.9$, *P. qionghdaoensis*) as well as clones identified with the KING toolset, we used VCFtools v0.1.15 (http://vcftools.sourceforge.net/man_latest.html) to calculate the mean depth of coverage and heterozygosity for each individual. The depth of coverage was relatively homogeneous (supplementary material, Fig. S3) and varied from 21× to 32×.

We used PLINK (Purcell, et al. 2007) to generate a variance-standardized relationship matrix for principal components analysis (PCA) and a distance matrix to build a neighbor joining tree (NJ-tree) with all filtered SNPs. The NJ tree was constructed using PHYLIP v.3.696 (<https://evolution.genetics.washington.edu/phylip.html>). Both PCA and NJ-tree analyses were performed based on the full set of SNPs. In addition, we used ADMIXTURE v1.3 for the maximum-likelihood estimation of individual ancestries (Alexander and Lange 2011). First, we generated the input file from a VCF containing unlinked SNPs. Besides, sites with missing data more than 30% have been filtered out. This analysis was run for K from 1 to 10, and the estimated parameter standard errors were generated using 200 bootstrap replicates. The best K was taken to be the one with the lowest cross-validation error. We also performed an IBD blocks analysis using BEAGLE v5.1 (Browning and Browning 2013) to detect identity-by-descent segments between pairs of species. The parameters we used are: window=100,000; overlap=10,000; ibdtrim=100; ibdlod=10.

Demographic trajectory reconstruction

To reconstruct the demographic history of *Populus* species, we first inferred the history of species splits and mixture based on genome wide allele frequency data using TreeMix v1.13 (Pickrell and Pritchard 2012). We removed the sites with missing data and performed linkage pruning. We then ran TreeMix implementing a default bootstrap and a block size of 500 SNPs ($-k=500$). The best migration edge was evaluated according to the greatest increase of total variation explained. The plotting R functions of the Treemix suite were then used to visualize the results.

Nucleotide diversity and divergence estimates

Nucleotide diversity, as well as relative and absolute divergence estimates were calculated based on genotype likelihoods. We used ANGSD v0.93 (<http://www.popgen.dk/angsd/index.php/ANGSD>) to estimate statistical parameters from the BAM files for all *Populus* species. First, we used ‘*dosaf 1*’ to calculate site allele frequency likelihood and then used ‘*realSFS*’ to estimate folded site frequency spectra (SFS).

Genome-wide diversity and Tajima's D were calculated with the parameter '*-doThetas 1*' in ANGSD based on the folded SFS of each species. We selected two population genomic statistics to estimate divergence F_{ST} and D_{XY} . We estimated SFS for each population separately and then used it as a prior to generate a 2D-SFS for each species pair. F_{ST} of each species pair were estimated with the parameters '*realSFS fst*' based on the 2D-SFS. Finally, we averaged the F_{ST} value of sites over 10kb windows. To estimate D_{XY} , we used ANGSD to calculate minor allele frequencies with the parameters '*-GL 1 -doMaf 1 -only_proper_pairs 1 -uniqueOnly 1 -remove_bads 1 -C 50 -minMapQ 30 -minQ 20 -minInd 4 -SNP_pval 1e-3 -skipTriallelic 1 -doMajorMinor 5*' and then computed D_{XY} as follows: $D_{XY} = A_1 * B_2 + A_2 * B_1$, with A and B being the allele frequencies of A and B, and 1 and 2 being the two populations. We averaged D_{XY} across 10kb windows.

To examine the relationships among diversity, differentiation, and recombination landscapes, we estimated Pearson's correlation coefficient between pairs of these statistics. These tests were performed across genomic windows for the 21 possible *Populus* species pairs. Finally, we used $d_a (D_{XY} - \text{mean } \pi)$ as a measure of divergence time.

Population-scale recombination rate and linkage disequilibrium

We estimated population scaled recombination rate with FastEPRR (Gao, et al. 2016) for each species separately. To eliminate the effect of sample size on the estimation of recombination rate, we downsampled to 13 randomly selected individuals for each species, corresponding to the number of individuals available for *Populus davidiana* (pdav). First, we filtered all missing and non-biallelic sites with VCFtools and then phased the data with the parameters "*impute=true nthreads=20 window=10,000 overlap=1,000 gprobs=false*" in Beagle v5.1 (Browning and Browning 2013). Finally, we ran FastEPRR v2.0 (Gao, et al. 2016) with a window size of 10kb. After getting the results, we estimated the correlation between recombination rate of one species to another. To evaluate LD decay, we used PLINK (Purcell, et al. 2007) to obtain LD statistics for each species. Parameters were set as follows: '*--maf 0.1 --r² gz --ld-window-kb 500 --ld-window 99999 --ld-window-r² 0*'. LD decay was finally plotted in R.

Divergent regions of exceptional differentiation

We further investigated genomic differentiation landscapes across multiple species pairs along the *Populus* divergence gradient and identified which evolutionary factors contribute to genomic differentiation. We reported genomic regions showing elevated or decreased values of F_{ST} , D_{XY} and π across 10kb windows. Windows falling above the top 5% or below the bottom 5% of F_{ST} and D_{XY} were considered. For these specific windows, we then classified them following the four models of divergence suggested by Irwin *et al.* 2018 and Han *et al.* 2017. These four models differ in the role of gene flow (with or without), or the type of selection (selective sweep, background selection or balancing selection).

Acknowledgements

We thank members of Jianquan Liu's lab for collecting samples and to Chris Cole for providing samples from *P. grandidentata*. Michael Barfuss and Elfi Grasserbauer provided assistance in the laboratory. Sequencing was performed at the Next Generation Sequencing Platform of the University of Berne and at the National Genomics Infrastructure (NGI) of Science for Life Laboratory, Stockholm. The Vienna Scientific Cluster (VSC) and the Swedish National Infrastructure for Computing (SNIC) at Uppsala Multidisciplinary Center for Advanced Computational Science (UPPMAX) provided access to computational resources. We are also grateful to members of the PopGen Vienna graduate school for helpful discussions. This manuscript is dedicated to the memory of our friend and colleague Prof. Christian Lexer.

Funding

This work was supported by a fellowship from the China Scholarship Council (CSC) to Huiying Shang, Swiss National Science Foundation (SNF) grant no.31003A_149306 to Christian Lexer, doctoral programme grant W1225-B20 to a faculty team including Christian Lexer, and the University of Vienna.

Conflict of interest disclosure

None of the authors have a conflict of interest to declare regarding the publication of this manuscript.

Data, script and code availability

The raw read data have been deposited with links to BioProject accession numbers PRJNA299390, PRJNA612655, PRJNA720790, and PRJNA297202 in the NCBI BioProject database (<https://www.ncbi.nlm.nih.gov/bioproject/>). All the scripts used for the analysis are available on: <https://doi.org/10.5281/zenodo.6785344>.

Supplementary information

Supplementary information is available in the “Supplementary material” section of the bioRxiv page of the article, <https://doi.org/10.1101/2021.08.26.457771>.

Author contributions

Study conceived and designed by Huiying Shang and Christian Lexer. Laboratory work conducted by Huiying Shang. Population genomic data analysis by Huiying Shang with feedback from Thibault Leroy. Interpretation of the results was undertaken by Huiying Shang, Martha Rendón-Anaya, Ovidiu Paun, David Field, Jaqueline Hess, Claus Vogl, Pär K. Ingvarsson, Christian Lexer and Thibault Leroy. The manuscript was drafted by Huiying Shang, with help from Thibault Leroy and Ovidiu Paun, and was improved and approved by all authors.

References

- Alexander DH, Lange K. 2011. Enhancements to the ADMIXTURE algorithm for individual ancestry estimation. *BMC Bioinformatics* 12:246.
- Booker TR, Keightley PD. 2018. Understanding the factors that shape patterns of nucleotide diversity in the house mouse genome. *Mol Biol Evol* 35:2971-2988.
- Browning BL, Browning SR. 2013. Improving the accuracy and efficiency of identity-by-descent detection in population data. *Genetics* 194:459-471.

- Burri R. 2017a. Dissecting differentiation landscapes: a linked selection's perspective. *J Evol Biol* 30:1501-1505.
- Burri R. 2017b. Interpreting differentiation landscapes in the light of long-term linked selection. *Evolution Letters* 1:118-131.
- Burri R, Nater A, Kawakami T, Mugal CF, Olason PI, Smeds L, Suh A, Dutoit L, Bureš S, Garamszegi LZ, et al. 2015. Linked selection and recombination rate variation drive the evolution of the genomic landscape of differentiation across the speciation continuum of *Ficedula* flycatchers. *Genome Res* 25:1656-1665.
- Charlesworth B, Campos JL. 2014. The relations between recombination rate and patterns of molecular variation and evolution in *Drosophila*. *Annu Rev Genet* 48:383-403.
- Charlesworth B, Morgan MT, Charlesworth D. 1993. The effect of deleterious mutations on neutral molecular variation. *Genetics* 134:1289-1303.
- Corbett-Detig RB, Hartl DL, Sackton TB. 2015. Natural selection constrains neutral diversity across a wide range of species. *PLoS Biol* 13:e1002112.
- Deacon NJ, Grossman JJ, Cavender-Bares J. 2019. Drought and freezing vulnerability of the isolated hybrid aspen *Populus x smithii* relative to its parental species, *P. tremuloides* and *P. grandidentata*. *Ecol Evol* 9:8062-8074.
- DePristo MA, Banks E, Poplin R, Garimella KV, Maguire JR, Hartl C, Philippakis AA, del Angel G, Rivas MA, Hanna M, et al. 2011. A framework for variation discovery and genotyping using next-generation DNA sequencing data. *Nat Genet* 43:491-498.
- Edelman NB, Frandsen PB, Miyagi M, Clavijo B, Davey J, Dikow RB, García-Accinelli G, Van Belleghem SM, Patterson N, Neafsey DE, et al. 2019. Genomic architecture and introgression shape a butterfly radiation. *Science* 366:594-599.
- Ellegren H, Smeds L, Burri R, Olason PI, Backström N, Kawakami T, Künstner A, Mäkinen H, Nadachowska-Brzyska K, Qvarnström A, et al. 2012. The genomic landscape of species divergence in *Ficedula* flycatchers. *Nature* 491:756-760.
- Gagnaire PA, Lamy JB, Cornette F, Heurtebise S, Dégremont L, Flahauw E, Boudry P, Bierne N, Lapègue S. 2018. Analysis of Genome-Wide Differentiation between Native and Introduced

- Populations of the Cupped Oysters *Crassostrea gigas* and *Crassostrea angulata*. *Genome Biol Evol* 10:2518-2534.
- Gao F, Ming C, Hu W, Li H. 2016. New Software for the Fast Estimation of Population Recombination Rates (FastEPRR) in the Genomic Era. *G3 (Bethesda)* 6:1563-1571.
- Han F, Lamichhaney S, Grant BR, Grant PR, Andersson L, Webster MT. 2017. Gene flow, ancient polymorphism, and ecological adaptation shape the genomic landscape of divergence among Darwin's finches. *Genome Res* 27:1004-1015.
- Harrison RG, Larson EL. 2016. Heterogeneous genome divergence, differential introgression, and the origin and structure of hybrid zones. *Mol Ecol* 25:2454-2466.
- Henderson EC, Brelsford A. 2020. Genomic differentiation across the speciation continuum in three hummingbird species pairs. *BMC Evol Biol* 20:113.
- Irwin DE, Milá B, Toews DPL, Brelsford A, Kenyon HL, Porter AN, Grossen C, Delmore KE, Alcaide M, Irwin JH. 2018. A comparison of genomic islands of differentiation across three young avian species pairs. *Mol Ecol* 27:4839-4855.
- Jansson S, Bhalerao R, Groover A. 2010. *Genetics and genomics of Populus*: Springer.
- Lamichhaney S, Berglund J, Almén MS, Maqbool K, Grabherr M, Martinez-Barrio A, Promerová M, Rubin CJ, Wang C, Zamani N, et al. 2015. Evolution of Darwin's finches and their beaks revealed by genome sequencing. *Nature* 518:371-375.
- Leroy T, Rougemont Q, Dupouey JL, Bodénès C, Lalanne C, Belser C, Labadie K, Le Provost G, Aury JM, Kremer A, et al. 2020. Massive postglacial gene flow between European white oaks uncovered genes underlying species barriers. *New Phytol* 226:1183-1197.
- Li H. 2013. Aligning sequence reads, clone sequences and assembly contigs with BWA-MEM. arXiv preprint arXiv:1303.3997.
- Li H, Handsaker B, Wysoker A, Fennell T, Ruan J, Homer N, Marth G, Abecasis G, Durbin R. 2009. The Sequence Alignment/Map format and SAMtools. *Bioinformatics* 25:2078-2079.
- Martin SH, Dasmahapatra KK, Nadeau NJ, Salazar C, Walters JR, Simpson F, Blaxter M, Manica A, Mallet J, Jiggins CD. 2013. Genome-wide evidence for speciation with gene flow in *Heliconius* butterflies. *Genome Res* 23:1817-1828.

- Martin SH, Davey JW, Salazar C, Jiggins CD. 2019. Recombination rate variation shapes barriers to introgression across butterfly genomes. *PLoS Biol* 17:e2006288.
- Martin SH, Jiggins CD. 2017. Interpreting the genomic landscape of introgression. *Curr Opin Genet Dev* 47:69-74.
- Martinsen GD, Whitham TG, Turek RJ, Keim P. 2001. Hybrid populations selectively filter gene introgression between species. *Evolution* 55:1325-1335.
- Nordborg M, Hu TT, Ishino Y, Jhaveri J, Toomajian C, Zheng H, Bakker E, Calabrese P, Gladstone J, Goyal R, et al. 2005. The pattern of polymorphism in *Arabidopsis thaliana*. *PLoS Biol* 3:e196.
- Nosil P, Feder JL. 2012. Widespread yet heterogeneous genomic divergence. *Mol Ecol* 21:2829-2832.
- Pickrell JK, Pritchard JK. 2012. Inference of population splits and mixtures from genome-wide allele frequency data. *PLoS Genet* 8:e1002967.
- Purcell S, Neale B, Todd-Brown K, Thomas L, Ferreira MA, Bender D, Maller J, Sklar P, de Bakker PI, Daly MJ, et al. 2007. PLINK: a tool set for whole-genome association and population-based linkage analyses. *Am J Hum Genet* 81:559-575.
- Rajora OP, Dancik BP. 1992. Genetic characterization and relationships of *Populus alba*, *P. tremula*, and *P. x canescens*, and their clones. *Theor Appl Genet* 84:291-298.
- Ravinet M, Yoshida K, Shigenobu S, Toyoda A, Fujiyama A, Kitano J. 2018. The genomic landscape at a late stage of stickleback speciation: High genomic divergence interspersed by small localized regions of introgression. *PLoS Genet* 14:e1007358.
- Renaut S, Grassa CJ, Yeaman S, Moyers BT, Lai Z, Kane NC, Bowers JE, Burke JM, Rieseberg LH. 2013. Genomic islands of divergence are not affected by geography of speciation in sunflowers. *Nat Commun* 4:1827.
- Renaut S, Owens GL, Rieseberg LH. 2014. Shared selective pressure and local genomic landscape lead to repeatable patterns of genomic divergence in sunflowers. *Mol Ecol* 23:311-324.

- Rennison DJ, Delmore KE, Samuk K, Owens GL, Miller SE. 2020. Shared patterns of genome-wide differentiation are more strongly predicted by geography than by ecology. *Am Nat* 195:192-200.
- Roux C, Fraïsse C, Romiguier J, Anciaux Y, Galtier N, Bierne N. 2016. Shedding light on the grey zone of speciation along a continuum of genomic divergence. *PLoS Biol* 14:e2000234.
- Schiffthaler B, Delhomme N, Bernhardsson C, Jenkins J, Jansson S, Ingvarsson P, Schmutz J, Street N. 2019. An improved genome assembly of the European aspen *Populus tremula*. bioRxiv:805614.
- Sendell-Price AT, Ruegg KC, Anderson EC, Quilodr an CS, Van Doren BM, Underwood VL, Coulson T, Clegg SM. 2020. The Genomic Landscape of Divergence Across the Speciation Continuum in Island-Colonising Silvereyes (*Zosterops lateralis*). *G3 (Bethesda)* 10:3147-3163.
- Shang H, Hess J, Pickup M, Field DL, Ingvarsson PK, Liu J, Lexer C. 2020. Evolution of strong reproductive isolation in plants: broad-scale patterns and lessons from a perennial model group. *Philos Trans R Soc Lond B Biol Sci* 375:20190544.
- Smith JM, Haigh J. 1974. The hitch-hiking effect of a favourable gene. *Genet Res* 23:23-35.
- Stankowski S, Chase MA, Fuiten AM, Rodrigues MF, Ralph PL, Streisfeld MA. 2019. Widespread selection and gene flow shape the genomic landscape during a radiation of monkeyflowers. *PLoS Biol* 17:e3000391.
- Stephan W. 2010. Genetic hitchhiking versus background selection: the controversy and its implications. *Philos Trans R Soc Lond B Biol Sci* 365:1245-1253.
- Stettler R, Bradshaw T, Heilman P, Hinckley T. 1996. *Biology of Populus and its implications for management and conservation*: NRC Research Press.
- Suarez-Gonzalez A, Hefer CA, Christe C, Corea O, Lexer C, Cronk QC, Douglas CJ. 2016. Genomic and functional approaches reveal a case of adaptive introgression from *Populus balsamifera* (balsam poplar) in *P. trichocarpa* (black cottonwood). *Mol Ecol* 25:2427-2442.
- Tavares H, Whibley A, Field DL, Bradley D, Couchman M, Copsey L, Elleouet J, Burrus M, Andalo C, Li M, et al. 2018. Selection and gene flow shape genomic islands that control floral guides. *Proc Natl Acad Sci U S A* 115:11006-11011.

- Tuskan GA, Difazio S, Jansson S, Bohlmann J, Grigoriev I, Hellsten U, Putnam N, Ralph S, Rombauts S, Salamov A, et al. 2006. The genome of black cottonwood, *Populus trichocarpa* (Torr. & Gray). *Science* 313:1596-1604.
- Van Belleghem SM, Cole JM, Montejó-Kovacevich G, Bacquet CN, McMillan WO, Papa R, Counterman BA. 2021. Selection and isolation define a heterogeneous divergence landscape between hybridizing *Heliconius* butterflies. *Evolution* 75:2251-2268.
- Vijay N, Bossu CM, Poelstra JW, Weissensteiner MH, Suh A, Kryukov AP, Wolf JB. 2016. Evolution of heterogeneous genome differentiation across multiple contact zones in a crow species complex. *Nat Commun* 7:13195.
- Wang M, Zhang L, Zhang Z, Li M, Wang D, Zhang X, Xi Z, Keefover-Ring K, Smart LB, DiFazio SP, et al. 2020. Phylogenomics of the genus *Populus* reveals extensive interspecific gene flow and balancing selection. *New Phytol* 225:1370-1382.
- Wu CI. 2001. The genic view of the process of speciation. *Journal of evolutionary biology* 14:851-865.
- Wolf JB, Ellegren H. 2017. Making sense of genomic islands of differentiation in light of speciation. *Nat Rev Genet* 18:87-100.
- Yamasaki YY, Kakioka R, Takahashi H, Toyoda A, Nagano AJ, Machida Y, Moller PR, Kitano J. 2020. Genome-wide patterns of divergence and introgression after secondary contact between *Pungitius* sticklebacks. *Philos Trans R Soc Lond B Biol Sci* 375:20190548.